Journal of Physics Communications

PAPER

Luminescence properties of pulsed laser deposited $CuIn_xGa_{1-x}Se_2$ films

Anna Zacharia[1], **Christiana Nicolaou**[2], **John Giapintzakis**[2] **and Grigorios Itskos**[1]

[1] Experimental Condensed Matter Physics Lab, Department of Physics, University of Cyprus, 75 Kallipoleos Av., PO Box 20537, 1678 Nicosia, Cyprus

[2] Department of Mechanical and Manufacturing Engineering, University of Cyprus, 75 Kallipoleos Av., PO Box 20537, 1678 Nicosia, Cyprus

E-mail: itskos@ucy.ac.cy

Keywords: CIGS films, pulsed laser deposition, photoluminescence, optical properties

OPEN ACCESS

RECEIVED
20 January 2020

REVISED
12 March 2020

ACCEPTED FOR PUBLICATION
23 March 2020

PUBLISHED
7 April 2020

Abstract

Pulsed laser deposition (PLD) of $CuIn_{1-x}Ga_xSe_2$ (CIGS) provides a low cost, single-step process via which stoichiometric, high quality thin films for light harvesting applications can be produced. Little is known about the optical properties of PLD-deposited CIGS and how they compare with the respected properties of the well-studied evaporated or sputtered CIGS films. We report herein a systematic spectroscopic investigation, probing the influence of PLD deposition temperature on the energetics and dynamics of emission from $CuIn_{0.7}Ga_{0.3}Se_2$ films. Variable-temperature steady-state and time-resolved photoluminescence in combination with Gaussian lineshape analysis allow us to unravel the contribution and nature of three main radiative channels, with the high energy one associated with electronic and two lower energy ones with defect levels. The analysis show that the band-edge luminescence grows at the expense of defect emission as PLD temperature increases in the 300 °C–500 °C range. This is further supported by: (i) The dramatic increase of the band-edge recombination lifetime from 30 to 180 ns, (ii) The quenching in the carrier trapping rate from 0.25 ns^{-1} to 0.09 ns^{-1} as growth temperature increases. The results correlate well with structural and electrical characterization studies reported previously on PLD-grown CIGS and rationally interpret the improvement in their optoelectronic properties as PLD deposition temperature increases .

1. Introduction

The quaternary semiconductor $CuIn_{1-x}Ga_xSe_2$ (CIGS) has been extensively studied in recent years as solar harvesting material owing to its material robustness, direct energy bandgap and strong absorption covering most of the visible solar spectrum [1, 2]. The high prospect of CIGS for thin film solar cells has been recently confirmed by the achievement of one of the highest efficiencies of 22.6% among all thin film solar cells at the laboratory level [3]. High quality CIGS films are typically fabricated via thermal co-evaporation [4] and sputtering techniques [5] however both of them exhibit certain drawbacks. They require precise control during deposition and typically a post-selenization step that is problematic due to the toxicity of materials used and non-uniformity of the layers it produces.

Pulsed laser deposition (PLD) is an alternative, relatively simple and low cost method that achieves good transfer of stoichiometry of the target composition [6]. PLD has been used to grow at a single-step process thin films of complex multinary compounds, however its use in the fabrication of CIGS films has been rather limited. We have recently demonstrated the fabrication of high-quality, nearly stoichiometric PLD-grown $CuIn_{0.7}Ga_{0.3}Se_2$ films using a systematic investigation of the PLD growth parameters [7]. The room temperature optical properties of such films were preliminary assessed and found optimized for substrate temperatures above 300 °C i.e. in the high temperature region of the growth temperature range probed. In particular a monotonic increase in the integrated PL intensity and a systematic decrease of the PL linewidth and Stokes shift was found as the deposition temperature was increased up to 500 °C. We preliminary attributed such observations to an

improved stoichiometry that results in an effective reduction of the band-edge potential fluctuations and the suppression of non-radiative recombination.

Within the present work, we expand our preliminary studies and report on a comprehensive luminescence investigation of $CuIn_{0.7}Ga_{0.3}Se_2$ films deposited at the optimum temperature region of 300 °C to 500 °C. The particular stoichiometry was selected for its suitability for high performance CIGS thin film solar cells [7–9]. By implementing sample temperature as the varying experimental parameter and Gaussian lineshape analysis, we monitor the energetics and dynamics of the various emissive channels in our films and we unravel their origin and contribution. Our work demonstrates the beneficial impact of increased PLD growth temperature on the optoelectronic properties of the studied films, resulting in smaller trapping rates, larger PL lifetimes and an overall increase of the band-edge relative to sub-gap emission.

2. Experimental details

CIGS films were deposited on soda-lime glass (SLG) substrates by PLD using a KrF excimer laser source ($\lambda = 248$ nm, $\tau \leqslant 25$ ns) in a high-vacuum chamber. The laser beam was driven through an arrangement of mirrors and focused by a focal lens on a polycrystalline $CuIn_{0.7}Ga_{0.3}Se_2$ (Testbourne) target at an incident angle of 45° inside the chamber. The target rotation during the irradiation ensured a uniform ablation of the target surface. The substrate was placed parallel to the surface target at a fixed distance of 4.5 cm. The deposition was carried out in the presence of background gas after the chamber was evacuated at a base pressure of 4×10^{-6} mbar. Argon (Ar) was used as background gas to confine the plume. The number of pulses and the repetition rate were kept constant at 6000 and 10 Hz respectively, for all depositions. Laser fluence, Ar background pressure and substrate temperature were systematically investigated in order to achieve the optimum growth conditions for high quality CIGS films. The assessment of the previous investigations related to fluence and background gas pressure have led to the selection of 1 J cm^{-2} and 0.01 mbar, respectively. All studied films are nearly stoichiometric with composition of $CuIn_{0.7}Ga_{0.3}Se_2$, and have been deposited at three substrate temperatures, namely 300 °C, 400 °C and 500 °C, being coded as CIGS 300 °C, CIGS 400 °C and CIGS 500 °C, respectively from here on.

Optical absorption was acquired via a triple-detector Perkin Elmer, Lamda 1050 spectrophotometer. Steady-state photoluminescence (PL) was excited via a 785 nm laser diode (Coherent StingRay) with a moderate power density of 50 mW-cm^{-2} and detected by a 0.75 m spectrometer (Acton750i Princeton) equipped with a liquid-nitrogen-cooled InGaAs array detector. Time-resolved photoluminescence (TR-PL) was measured using a spectrometer-based (FluoroLog FL3 Horiba Jobin Yvon) time correlated single photon counting (TCSPC) method, by exciting the sample with a 785 nm pulsed laser (DeltaDiode-785L) with a pulse width of ~80 ps. The average PL lifetime t_{avg} of the PL decays was calculated from the relation:

$$t_{avg} = \frac{\sum_i A_i \tau_i^2}{\sum_i A_i \tau_i} \tag{1}$$

where τ_i are the decay times extracted from multi-exponential fits of the PL transients and A_i the corresponding decay amplitudes. Temperature-dependent steady-state and time-resolved PL measurements were carried out in the 10–300 K and 77–300 K range by placing the samples in the cold finger of a Janis CCS-150 closed-cycle refrigerator and a Janis VPF liquid nitrogen optical cryostat, respectively. To resolve the PL dynamics of mixtures of luminescence species with overlapping spectra, a variation of the technique known as time-resolved emission spectra (TRES) was employed. A typical TRES measurement involves moving the monochromator in fixed wavelength steps, with time-resolved decays acquired at each wavelength. With this process, a three-dimensional graph of PL intensity versus wavelength and time can be obtained. It is possible to obtain 'slices' of data in the intensity–wavelength plane to obtain the time-evolution of PL spectra at different times during the decay.

3. Results and discussion

The temperature-dependent PL spectra of the studied CIGS films in the 10–300 K range and the respective absorption spectral profiles at 300 K are displayed in figure 1. A room temperature bandgap in the vicinity of ~1.2 eV can be estimated using the first derivative maxima that slightly blue-shifts by as much as ~20 meV as PLD deposition temperature increases due to strain relief of the chalcopyrite crystal structure [7, 10]. All films exhibit broad, multi-peak PL in the near-IR with similar spectral characteristics to those reported for material produced via evaporation [11] or PLD [12]. Inspection of the PL spectra reveals a weakly-temperature sensitive high energy emission peaked at ~1.1–1.15 eV and a strongly temperature-dependent contribution at lower energies.

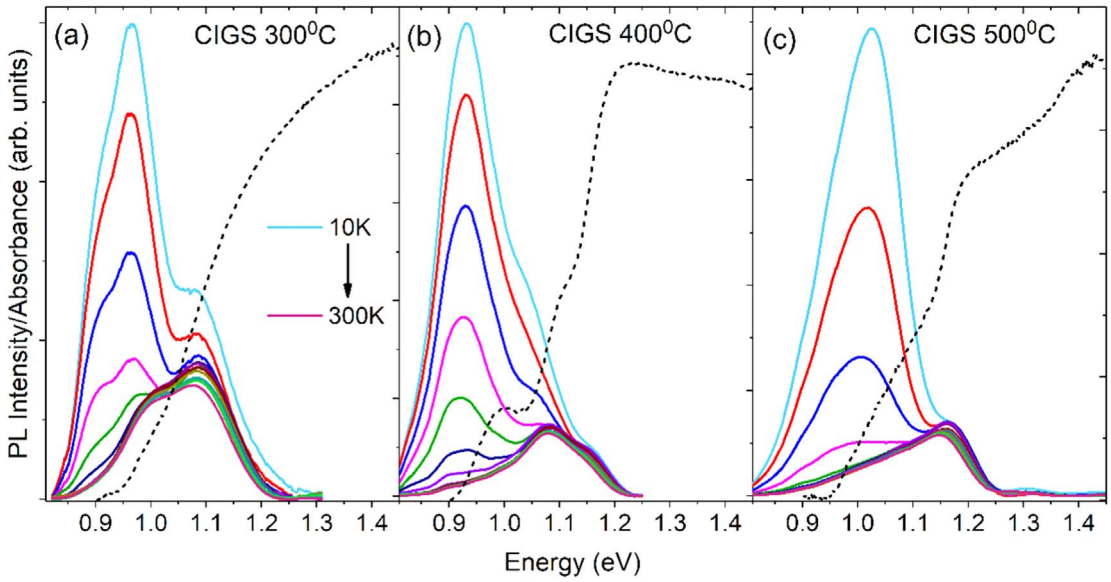

Figure 1. Room-temperature absorption (dotted lines) and temperature-dependent PL spectra of (a) CIGS 300 °C, (b) CIGS 400 °C and (c) CIGS 500 °C in the 10–300 K range.

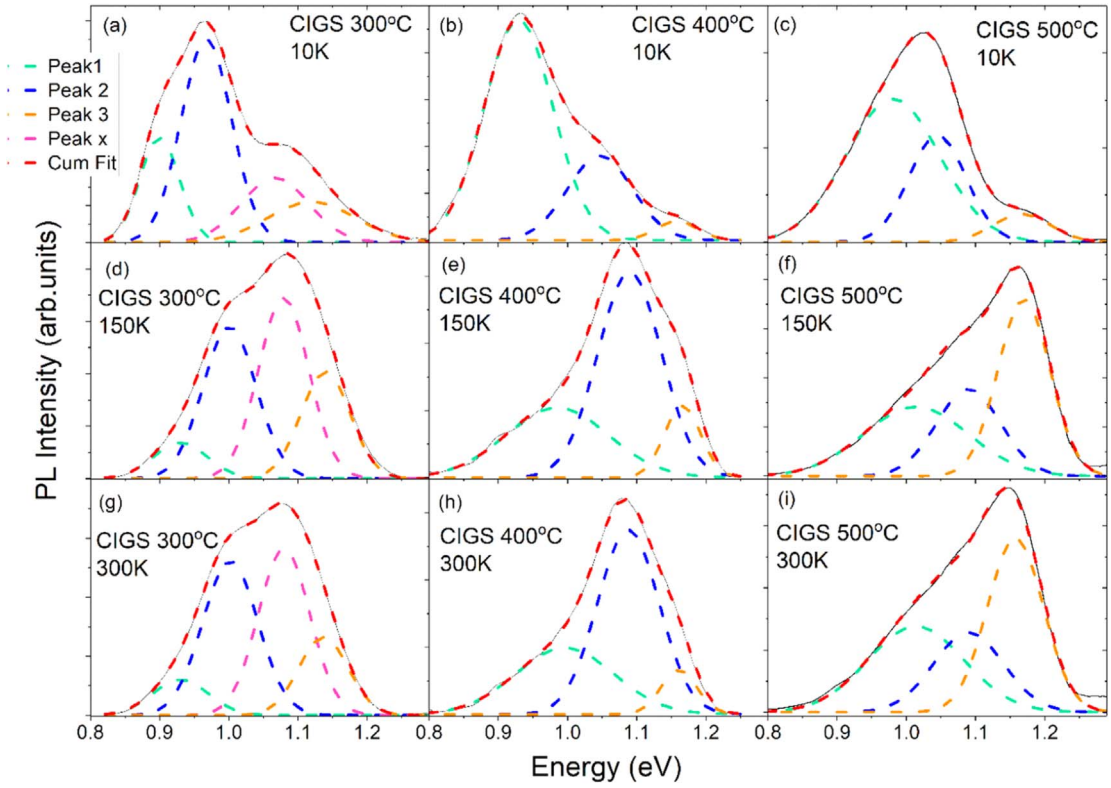

Figure 2. Representative examples of Gaussian lineshape analysis of the PL spectra of CIGS300 °C, CIGS400 °C and CIGS500 °C at temperatures of 10, 150 and 300 K.

Figure 2 contains representative Gaussian curve fits of the PL at three temperatures per film. CIGS 400 °C and CIGS 500 °C can be consistently fited with three Gaussian peaks (Peaks 1,2,3 in ascending energy) while an additional peak (Peak x) is required to simulate the PL spectrum of CIGS 300 °C at all temperatures.

At room temperature the high energy peak 3 in the films blue shifts with substrate temperature from ~1.14 eV at 300 °C to ~1.16 eV at 500 °C, in similar fashion and magnitude to the strain-induced shift of the energy gap observed in the optical absorption data. Furthermore its intensity shows significantly weaker dependence on temperature compared to the lower energy peaks. Based on the energetic proximity to the band-

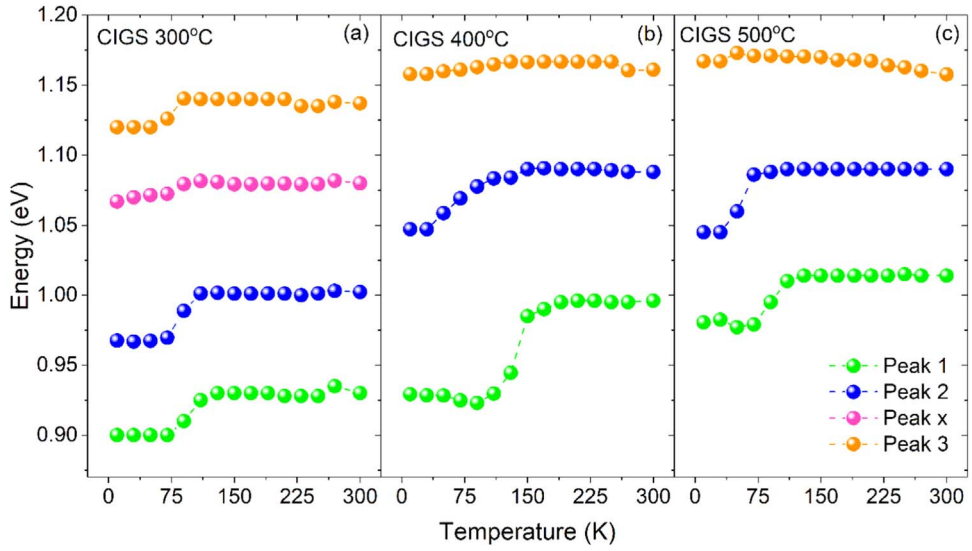

Figure 3. Energy positions of the extracted Gaussian PL peaks in the 10–300 K range for samples: (a) CIGS 300 °C, (b) CIGS 400 °C, (c) CIGS 500 °C.

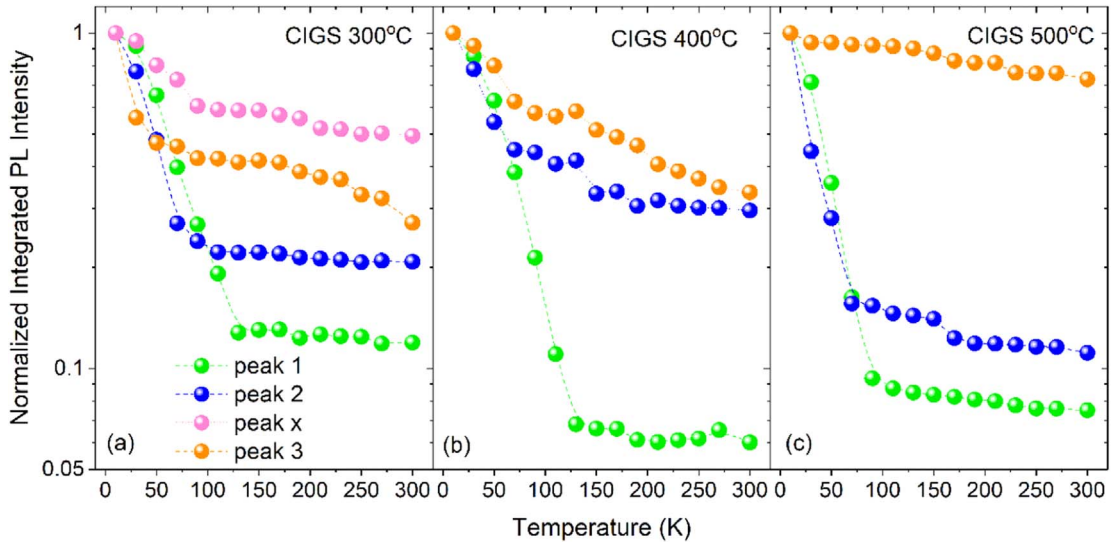

Figure 4. Integrated PL Intensity of the Gaussian peaks in the 10–300 K range from: (a) CIGS 300 °C, (b) CIGS 400 °C, (c) CIGS 500 °C. The PL intensity has been normalized to the intensity maximum that occurs for each film/peak at the lower temperature probed i.e. 10 K.

edge, the similar shift it exhibits with growth temperature and its weak temperature dependence, we assign peak 3 to the band-to-band CIGS radiative transition.

Lower energy peaks 1 and 2 are found at energies of ~150–240 meV and ~60–150 meV below the band-to-band emission, respectively with the separation from the band-edge decreasing as deposition temperature increases, as seen in figure 3.

This indicates that the position of the deep levels is influenced by the PLD temperature, with higher deposition temperatures inducing somewhat shallower defect levels. Peak 1, to a larger degree, as well as peak 2 exhibit strong quenching as temperature increases up to ~130 K in all films as seen in figure 4 combined with a concomitant anomalous temperature-dependent blue shift in the 80–150 K range, as observed in figure 3. Such behaviour reported previously in co-evaporated CIGS thin films [11], indicates that carriers experience a relatively low trapping potential at the defect deep levels; as temperature increases carriers acquire sufficient energy to become detrapped and redistribute at higher energy local minima of the manifold of the defect states where they recombine non-radiatively, blue shifting and quenching the respective emission peaks. A similar type of blue-shift across the same temperature range is also visible in the band-to-band peak (peak 3) of the CIGS

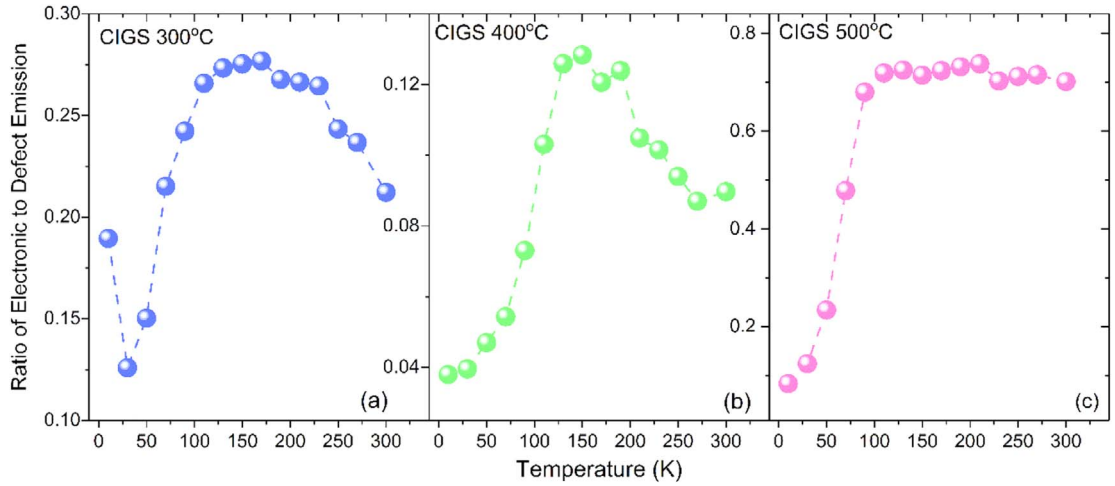

Figure 5. Ratio of integrated area of peak 3 (band-to-band) to the integrated emission from lower energy peaks (defect-based) at different temperatures in the range of 10–300 K range for the (a) CIGS300 °C, (b) CIGS400 °C and (c) CIGS500 °C films.

300 °C film which can be analogously being assigned to thermally-activated redistribution of carriers within energy local minima of the band potential fluctuations. Such behaviour is not observed at the band-edge emission peak of CIGS 400 °C and 500 °C films which confirms the hypothesis of improved compositional uniformity at higher PLD temperatures [7] resulting in an effective reduction of the band-edge potential fluctuations.

An assignement of the deep levels participating in the emissive peaks 1 and 2 on specific CIGS point defects is challenging due to the spatial and energetic disorder that broadens deep levels to a manifold of states as evidenced by the associated broad luminescence peaks. Defects with the lower formation energy in CIGS are I_{Cu} (interstitials) and V_{Cu} (vacancies) acting as individual donor and acceptors, respectively or correlated $In_{Cu}+V_{Cu}$ defect complexes [13, 14]. The latter complex induces a donor-to-acceptor emission at roughly ~200 meV below the gap [14] that based on the energetics may be associated with peak 1. According to our previous work [7], the films are slightly In-rich and Ga-deficient so In interstitials and/or Ga vacancies are also candidate deep levels involved on the emissive peaks 1 and 2. Peak x that appears as a fourth Gaussian to properly model the emission from CIGS 300 °C probably originates on a secondary $Cu_{2-x}Se$ phase observed at low PLD-growth temperatures [7]. Such assignement seems to be supported by the observation of an indirect $Cu_{2-x}Se$ electronic gap at energies coincident with peak x [15], and the absence of the peak at higher PLD deposition temperatures in which such secondary phase diminishes.

Based on the aforementioned assignments the ratio of band-to-band (peak 3) to defect (peak 1 + peak 2 + peak x) integrated emission for the three films in the range of 10 K to 300 K is displayed in figure 5. The higher emission quenching rate of the defect related peaks effectively increases the ratio from 10 K to 100–130 K while a decrease of the ratio is observed for temperatures higher than 200 K for CIGS300 °C and CIGS400 °C, as temperature-activated trapping quenches the band-to-band peak in favor of deep level emission. For CIGS500 °C an impressive dominance of the band-to-band recombination is observed for sample temperatures higher than 100 K with peak emission almost an order of magnitude higher than that of CIGS300°C and no sign of temperature-activated quenching up to room temperature, confirming the improvement on the optoelectronic properties of the film.

Additional information on the recombination mechanisms is provided by the temperature-dependent carrier dynamics probed via time-resolved PL experiments. For all peaks 1,2 and 3 monitored at each temperature in the 80–300 K range, the PL decays require modelling by a complex triple exponential function. Initially the PL dynamics are globally quantified for each Gaussian peak by its respective average PL lifetime, extracted by the amplitudes and lifetimes of each of the three exponential decays, as shown in equation (1). Representative transients at 80 K, 180 K and 300 K monitoring the dynamics of the band-to-band peak 3 for each sample, along with the respective exponential fits and the average PL lifetimes are displayed in figure 6.

Figure 7 contains the extracted average PL lifetime versus temperature for peaks 1,2,3 of the the three films. The general trend observed is that the average PL lifetime: (i) increases as lower energy peaks are probed, (ii) reduces with sample temperature for each peak, (iii) reduces per peak as higher PLD temperatures are employed. Trends (i) and (ii) are generally consistent with the assignment of the high/low energy emission to electronic/defect-based transitions respectively. Band-edge transitions are generally expected to exhibit larger recombination rates compared to sub-gap transitions due to higher radiative rates and the presence of non-

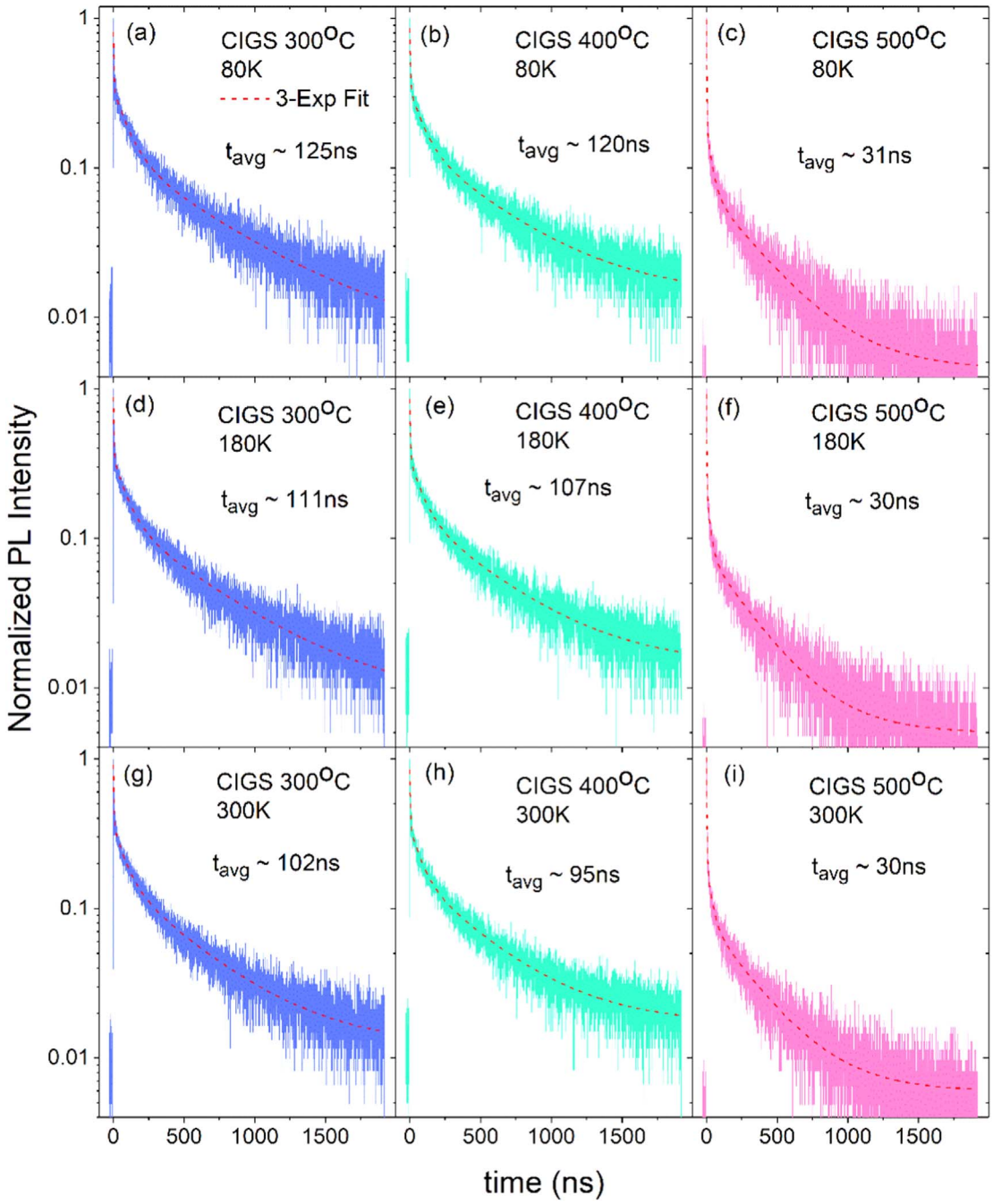

Figure 6. Representative PL decay curves, triple exponential fits and calculated average PL lifetimes for the band-to-band peak (peak 3) of the three CIGS film emission at (a)-(c) 80 K, (d)-(f) 180 K and (g)-(i) 300 K.

radiative trapping channels that feed the lower energy peaks and effectively quench the higher energy emission lifetime. Furthermore increase of the temperature typically benefits non-radiative quenching over radiative recombination [14, 16]. Interpretation of trend (iii) requires more elaborate thinking. For defect-related peaks 1 and 2, the shortening of the radiative rate as PLD deposition temperature increases, may be attributed to slightly shallower defect states being involved in the sub-gap emission, as hinted by the smaller separation of peaks 1,2 compared to the band-edge peak 3, seen in figure 3. On the other hand, the quenching of the band-edge PL lifetime appears rather contradictory to the steady-state PL results that indicate a monotonic increase in the integrated PL intensity as deposition temperature is increased up to 500 °C. Furthermore, the average PL lifetime values obtained for the band-to-band peak 3 appear reasonable only for CIGS500 °C, being comparable to values reported in literature for high quality CIGS thin films [16, 17] while the dynamics of such peak appear significantly inflated for the CIGS300 °C and CIGS400 °C films.

The larger band-to-band PL lifetimes obtained are in fact an artifact as the transients monitor effectively the convolution of peak 3 with the lower peak 2 or peak x; such overlap for CIGS300 °C and CIGS400 °C films is

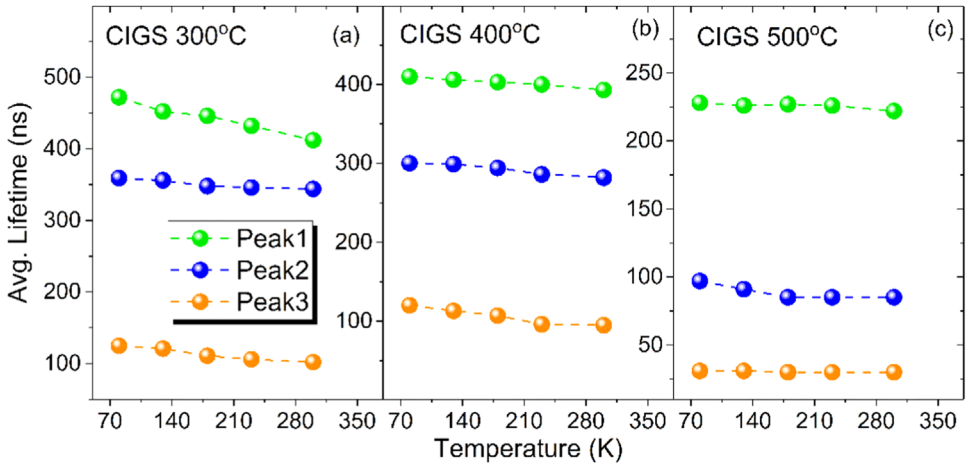

Figure 7. Average PL lifetime versus temperature in the 80–300 K range for the three emissive contributions of: (a) CIGS300 °C, (b) CIGS400 °C and (c) CIGS500 °C.

substantial, as vividly observed in figure 2. To avoid such artifacts we employ a more elaborate method in which we obtain emission transients across the whole PL lineshape and we reconstruct the temporal evolution of the PL spectra. Each of the spectra on this time sequence are linefitted with the three (or four for CIGS 300C) Gaussian peaks and the integrated area of each of the Gaussians is plotted versus time (TRES spectra). Figure 8 contains the results of such analysis. Due to the intensive analysis associated with such method, we focus our discussion solely at room temperature.

The obtained decays can now be adequately fitted using double-exponential decays, with a long lifetime of hundreds of ns and a significant shorter decay of the order of few to tens of ns. It is evident that the method introduces a large statistical uncertainty in the extracted decay lifetimes due to the small density of experimental data but circumvents the significant systematic error produced by the spectral overlap of the Gaussian peaks; the validity of the method has been demonstrated in previous work of some of the manuscript authors on probing the dynamics of multi-component emission with overlapping peaks [16, 18].

For the rest of the manuscript, we focus our discussion on the room temperature band-to-band PL dynamics. The TRES analysis yields an average PL lifetime that increases by an order of magnitude i.e. from ~4 ns to ~40 ns, as PLD temperature increases, in close agreement with the order of magnitude intensity enhancement observed in the steady-state PL results and consistent with the lifetime range values reported in the literature. The short τ_{short} and long τ_{long} lifetimes of the bi-exponential decay and the relative amplitude ratio of the latter to the former are displayed in table 1.

The two lifetimes increase while the relative contribution of the long decay component enhances by more than an order of magnitude as the substrate temperature increases from 300 to 400, 500 °C. Taking into account the concomitant increase of the band-edge emission, observed mainly at the higher deposition temperature, we tentatively assign τ_{short} to non-radiative recombination associated with trapping of carriers at the deep levels while τ_{long} is associated with the dynamics of the band-to-band transition. Trapping times of the order of few ns and band-to-band recombination of the order of tens to hundreds of ns such as those observed in our films, have been routinely reported in the literature for evaporated CIGS films [13, 15, 17, 19] so such assignment appears reasonable. It is noted that within the low excitation level range of 1 to 25 μW employed in our TCSPC experiments, no influence of the excitation fluence was observed in PL dynamics, which suggests that defect saturation effects by carriers is absent [13, 15].

4. Conclusions

A systematic spectroscopic investigation of PLD-deposited CIGS films is reported. Our studies probe the influence of PLD deposition temperature on the emission properties of such solids and map the energetics and dynamics of the electronic and defect radiative transitions. Variable-temperature steady-state and time-resolved experiments in combination with Gaussian lineshape analysis allow us to unravel the contribution of three main radiative channels, with the high energy one associated with electronic and two lower energy ones with defect CIGS levels. The work demonstrates that important figures of merit for the implementation of such films in solar cell applications improve as PLD temperature increases in the 300 °C–500 °C range. In particular, we observe a 3-fold increase in the carrier trapping time, a 6-fold increase in the band-edge recombination time and

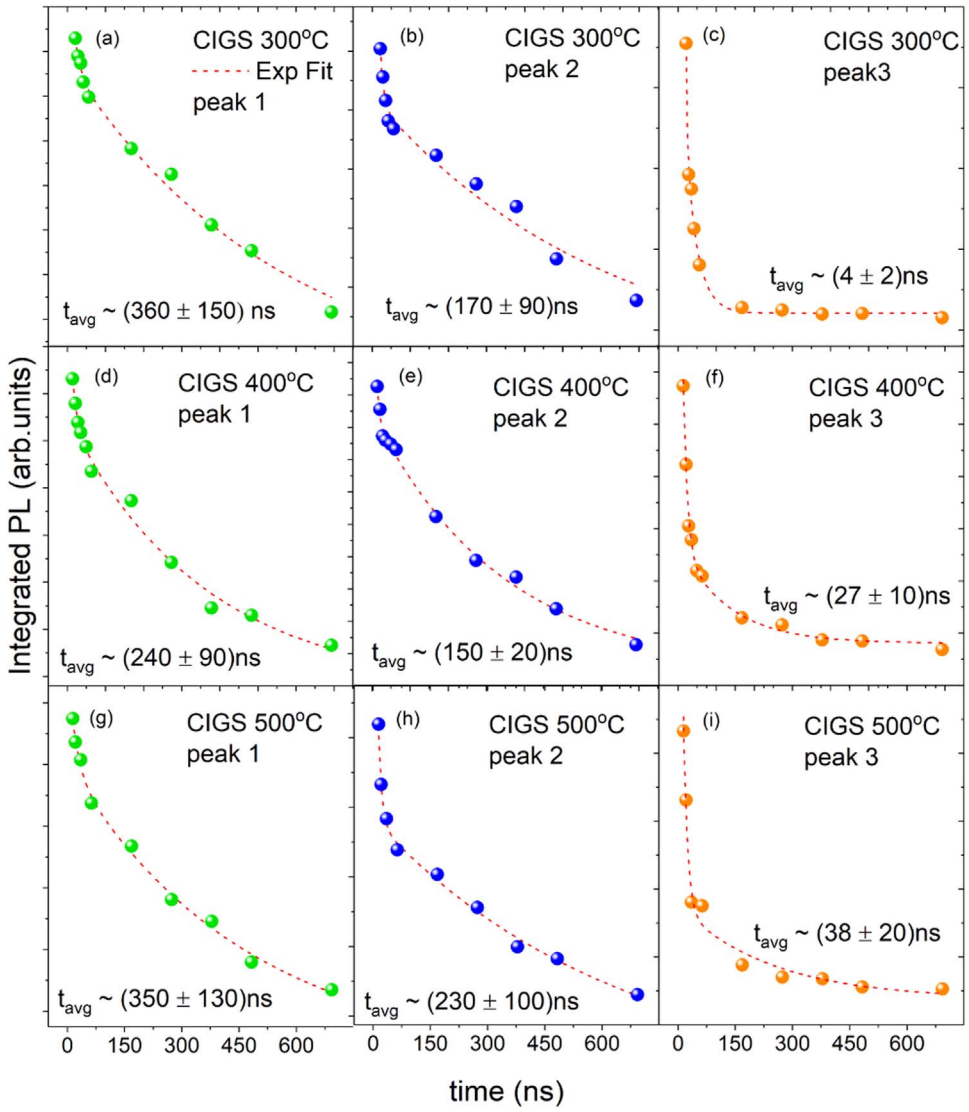

Figure 8. Time evolution of the integrated emission for the three main Gaussian PL contributions of the CIGS films obtained by analysis of TRES experiments at room temperature.

Table 1. Parameters of the biexponential decay fit of the TRES PL data for the band-to-band peak (Peak3).

Sample	τ_{short} (ns)	τ_{long} (ns)	$\frac{A_{long}}{A_{long}+A_{short}}$
CIGS 300C	4	30	0.01
CIGS 400C	10	130	0.14
CIGS 500C	11	180	0.16

a 3-fold enhancement in the ratio of electronic to defect emission. Such values are not far from those reported in well-studied, state-of-the-art evaporated or sputtered CIGS films, confirming the prospect of PLD as fabrication method for high quality CIGS material.

Acknowledgments

This work was co-funded by the European Regional Development Fund and the Republic of Cyprus through the Cyprus Research and Innovation Foundation (Project: EXCELLENCE/1216/ 0232)

ORCID iDs

Grigorios Itskos https://orcid.org/0000-0003-3971-3801

References

[1] Ramanujam J and Singh U P 2017 Copper indium gallium selenide based solar cells—a review *Energy Environ. Sci.* **10** 1306–19
[2] Lee T D and Ebong A U 2017 Review of thin film solar cell technologies and challenges *Renew. Sustain. Energy Rev.* **70** 1286–97
[3] SolarFrontier 2017 Solar Frontier Achieves World Record Thin-Film Solar Cell Efficiency of 22.9%(http://solar-frontier.com/eng/news/2017/1220_press.html)
[4] Marudachalam M, Birkmire R, Hichri H, Schultz J, Swartzlander A and Al-Jassim M 1997 Phases, morphology, and diffusion in $CuIn_xGa_{1-x}Se_2$ thin films *J. Appl. Phys.* **82** 2896–905
[5] Frantz J A, Bekele R Y, Nguyen V Q, Sanghera J S, Bruce A, Frolov S V, Cyrus M and Aggarwal I D 2011 $Cu(In,Ga)Se_2$ thin films and devices sputtered from a single target without additional selenization *Thin Solid Films* **519** 7763–5
[6] Schou J 2009 Physical aspects of the pulsed laser deposition technique: The stoichiometric transfer of material from target to film *Appl. Surf. Sci.* **255** 5191–8
[7] Nicolaou C, Zacharia A, Itskos G and Giapintzakis J 2018 Influence of process parameters on the properties of pulsed laser deposited $CuIn_{0.7}Ga_{0.3}Se_2$ thin films *Sol. Energy* **174** 793–802
[8] Contreras M A, Ramanathan K, AbuShama J, Hasoon F, Young D L, Egaas B and Nouf R 2005 Diode Characteristics in State-of-the-Art ZnO/CdS/ $Cu(In_{1-x}Ga_x)Se_2$ Solar Cells *Prog. Photovolt: Res. Appl.* **13** 209–16
[9] Jackson P, Hariskos D, Lotter E, Paetel S, Wuerz R, Menner R, Wischmann W and Powalla M 2011 New world record efficiency for $Cu(In,Ga)Se_2$ thin-film solar cells beyond 20% *Prog. Photovolt: Res. Appl.* **19** 894–7
[10] Theodoropoulou S, Papadimitriou D, Mamalis A, Manolakos D, Klenk R and Lux-Steiner M–C 2007 Band-gap energies and strain effects in $CuIn_{1-x}Ga_xS_2$ based solar cells *Semicond. Sci. Technol.* **22** 933
[11] Liao Y-K *et al* 2012 Observation of unusual optical transitions in thin-film Cu(In,Ga)Se2 solar cells *Optic. Express* **20** A836–42
[12] Chen S-C *et al* 2014 Growth and characterization of $Cu(In,Ga)Se_2$ thin films by nanosecond and femtosecond pulsed laser deposition *Nanoscale Res. Lett.* **9** 280
[13] Siebentritt S, Igalson M, Persson C and Lany S 2010 The electronic structure of chalcopyrites—bands,point defects and grain boundaries *Prog. Photovolt: Res. Appl.* **18** 390–410
[14] Yang J, Du H W, Li Y, Gao M, Wan Y Z, Xu F and Ma Z Q 2016 Structural defects and recombination behavior of excited carriers in $Cu(In,Ga)Se_2$ solar cells *AIP Adv.* **6** 085215
[15] Ghosh A, Kulsi C, Banerjee D and Mondal A 2016 Galvanic synthesis of Cu_{2-X} Se thin films and their photocatalytic and thermoelectric properties *Appl. Surf. Sci.* **369** 525–34
[16] Maiberg M, Hölscher T, Zahedi-Azad S, Fränzel W and Scheer R 2015 Investigation of long lifetimes in $Cu(In,Ga)Se_2$ by time-resolved photoluminescence *Appl. Phys. Lett.* **107** 122104
[17] Shimakawa S-I, Kitani K, Hayashi S, Satoh T, Hashimoto Y, Takahashi Y and Negami T 2006 Characterization of Cu(In,Ga)Se2 thin films by time-resolved photoluminescence *Phys. Stat. Sol.* (a) **203** 2630–3
[18] Papagiorgis P, Stavrinadis A, Othonos A, Konstantatos G and Itskos G 2016 The Influence of doping on the optoelectronic properties of PbS colloidal quantum dot solids *Sci. Rep.* **6** 18735
[19] Maiberg M, Hölscher T, Jarzembowski E, Hartnauer S, Zahedi-Azad S, Fränzel W and Scheer R 2017 Verification of minority carrier traps in $Cu(In,Ga)Se_2$ and $Cu_2ZnSnSe_4$ by means of time-resolved photoluminescence *Thin Solid Films* **633** 208–12